

¹A. K. Dutta, Phys. Rev. C 3, 480 (1971).

²A. K. Dutta, Progr. Theoret. Phys. (Kyoto) 39, 1069 (1968).

³L. A. König, J. H. Mattauch, and A. H. Wapstra, Nucl. Phys. 31, 18 (1962).

⁴*Nuclear Data Sheets*, compiled by K. Way *et al.* (Printing and Publishing Office, National Academy of Sciences – National Research Council, Washington, D. C.).

⁵I. Tami and I. Unna, Ann. Rev. Nucl. Sci. 10, 353 (1960); B. F. Bayman, A. S. Reiner, and R. K. Sheline, Phys. Rev. 115, 1627 (1959); A. Bohr and B. R. Mottelson, Kgl. Danske Videnskab. Selskab; Mat.-Fys. Medd. 27, No. 16 (1953); K. Adler, A. Bohr, T. Huns, B. R. Mottelson, and A. Winther, Rev. Mod. Phys. 28, 432 (1956).

⁶N. Bohr, Nature 137, 344 (1936); F. L. Friedman and V. F. Weisskopf, *The Compound Nucleus; Niels Bohr and The Development of Physics* (Pergamon Press, New York, 1955), p. 134.

⁷C. W. Li, W. Wahling, W. A. Fowler, and C. C. Lauritsen, Phys. Rev. 83, 512 (1951); D. M. Van Patter and W. Wahling, Rev. Mod. Phys. 26, 402 (1954); F. Ajzenberg and T. Lauritsen, *ibid.* 24, 321 (1952); 27, 77 (1955); Nucl. Phys. 11, 1 (1959); T. Lauritsen and F. Ajzenberg, Ann. Rev. Nucl. Sci. 10, 409 (1961).

⁸E. Fermi, Z. Physik 88, 161 (1934); R. D. Albert and C. S. Wu, Phys. Rev. 74, 876 (1948).

⁹*Nuclear Spectroscopy*, edited by F. Ajzenberg-Selove (Academic Press Inc., New York, 1960), p. 165.

Analyses of Elastic Proton-Alpha Scattering*

Richard A. Arndt, L. David Roper, and Robert L. Shotwell

Virginia Polytechnic Institute and State University, Blacksburg, Virginia 24061

(Received 15 June 1970; revised manuscript received 20 January 1971)

Starting from reported single-energy analyses of p - α elastic scattering we obtain an energy-dependent solution to p - α scattering between 0 and 23 MeV. We also did single-energy analyses at energies where both differential-cross-section and polarization data are available starting from the energy-dependent solution. The single-energy results are rather erratic, but tend to lie near the energy-dependent result.

INTRODUCTION

In a recent paper¹ we have reported elastic energy-dependent n - α scattering analyses. The results did not completely agree with the p - α analyses that were then available. In the present paper we report similar energy-dependent p - α scattering analyses.

The p - α phases available at the beginning of the analyses reported here fell into essentially two visually different solutions which we label solutions A and B. Solution B contains the latest single-energy analyses results. (See Fig. 2 and Fig. 3 for phase shifts and references.) (We have not used all available single-energy phase shifts in defining solutions A and B, we have only used those which visually fell into a fairly smooth curve for each solution and only the minimum number needed to adequately define the curves.) We fit our energy-dependent parametrization (see below) to these two solutions to use as input in our analyses. We found that starting from solution B, which includes the most recent single-energy analyses, led to the best fit to all of the data. However, the final solution differs considerably from both of the input solutions.

Starting from the energy-dependent solution we

did single-energy analyses at energies where both differential cross-section and polarization data are available. The resulting phase shifts are erratic, but tend to lie near the energy-dependent result.

The main features of our solution are: (a) the $S_{1/2}$ is approaching -93° near 23 MeV; (b) the $P_{1/2}$ peaks at $\sim 57^\circ$ at 12 MeV, and then falls back to $\sim 50^\circ$ at 23 MeV; (c) the $P_{3/2}$ resonates at ~ 2.8 MeV, peaks at $\sim 114^\circ$ at 5.8 MeV, and then passes back through 90° at ~ 21 MeV; (d) the $D_{3/2}$ rises very rapidly to $\sim 10^\circ$ between 19 and 23 MeV, apparently to resonate just above the d -He³ threshold; (e) the $D_{5/2}$ rises rapidly to $\sim 8^\circ$ between 17 and 23 MeV; (f) the $F_{5/2}$ rise to 1.5° at 23 MeV; and (g) the $F_{7/2}$ rises to 2° at 23 MeV.

DATA

Only two of the four possible angular observables² have been measured for the p - α system. References for the available p - α data up to 30 MeV are given in the Appendix.

We use the data selection criteria outlined in our previous paper on n - α scattering¹:

In collections of experimental scattering data there are always redundancies and inconsistencies.

It is incumbent upon the analyzer of scattering data to cull out "bad data" and redundant data, the latter being necessary because of limitations on computer time.

Inconsistent data are most safely culled by simultaneously considering all of the data over the selected energy range, and culling out those experiments that are obviously inconsistent with the entire body of data. This is done before an analysis begins or very early in the analysis. Later in the analysis, as unique solutions are (hopefully) obtained, these solutions can be cautiously used to point out finer inconsistencies in the data. Ideally, these fine inconsistencies should be checked out by further experimental measurements.

Careful reading of experimental papers and communications with the experimentalists are indispensable in culling out redundant data. A few general rules are applicable with caution: (1) Experimentalists often report preliminary data which are later superceded by their final data; (2) new data generally should have preference over old data; and (3) more precise data generally should have precedence over less precise data. We now apply the above principles and cull the elastic p - α scattering data.

A. Differential Cross Sections

We discard the data at 3.03 (Data Reference D16) and 3.04 MeV (D2) because there are later, more precise data at 3.006 MeV (D19). Likewise, we discard the data at 3.58 MeV (D2) because of data at 3.51 MeV (D16); data at 4.02 MeV (D16) because of data at 4.006 MeV (D19); data at 5 MeV (D16) because of data at 5.011 MeV (D19); and data at 9.55 MeV (D8) because of data at 9.48 MeV (D4) and at 9.76 (D9). (Also, the latter two agree better than do either of the latter two with the former.)

There are large disagreements among data at 4.8 MeV (D3) and data at 4.5 MeV (D16) and 5 MeV (D16); among data at 5.1 MeV (D3) and data at 5 MeV (D16) and 5.011 MeV (D19); and among data at 9.73 MeV (D7) and data at 9.76 MeV (D9). Therefore, we discard the 4.8, 5.1, and 9.73 MeV data.

Data discarded simply because of redundancy are at 14.49 MeV (D15) and 14.38 MeV (D15) because of data at 14.28 MeV (D22) and 14.32 MeV (D18).

A datum at 19.5 MeV (D5) greatly disagrees with the data at 20.1 MeV (D17). The 19.5 MeV datum is discarded.

B. Polarization

The one datum at 1.375 MeV (P5) is discarded because it is consistent with data at 1.35 MeV (P17). Likewise, we discard the one datum at 2.02 MeV (P5) because of data at 1.97 MeV (P17), the one datum at 2.13 MeV (P14) because of data at 2.18 MeV (P17), and one datum at 3.01 MeV (P14) because of data at 3.00 MeV (P17), the one datum at 4.18 MeV (P14) and the data at 4.16 MeV (P13) because of data at 4.15 MeV (P16).

The one datum at 7.9 MeV (P6) is discarded because it is much less precise than and is consistent with data at 7.87 MeV (P10) and 7.89 MeV (P23).

Near 10 MeV there are four sets of measurements. One 10-MeV set (P7) is inconsistent with the other three sets at certain angles. The other two sets [9.82, 9.84, and 9.89 MeV (P10) and 10 MeV (P21)] do not overlap and, therefore, cannot be checked for consistency. We discard the P7 10-MeV data.

The data at 12.04 MeV (P22) are more precise than and consistent with the data at 11.9 MeV (P10) and at 11.94 MeV (P23). We, therefore, discard the data at 11.9 and 11.94 MeV to reduce redundancy.

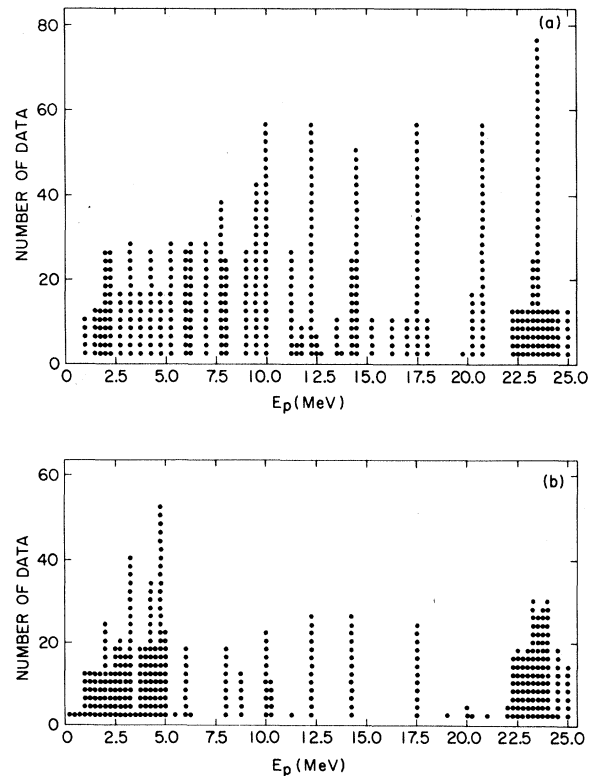


FIG. 1. Data that remained after selection criteria were applied. (a) Differential-cross-section data. (b) Polarization data.

The data at 14.23 MeV (P22) are much more precise and smoothly varying with angle than are the data at 14.5 MeV (P9). The two sets are inconsistent for about half of the 14.5-MeV data points. We discard the 14.5-MeV data. The datum at 14.4 MeV (P6) is consistent with and much less precise than the 14.23-MeV data (P22); thus we discard it.

Data at 17.47, 17.51, 17.52, and 17.54 MeV (P15) are consistent with more precise data at 17.45 MeV (P22). Therefore, we discard these data to reduce redundancy.

The remaining data are distributed as shown in Fig. 1.

ENERGY PARAMETRIZATION AND LEAST-SQUARES FITS

The parametrization that we use for the phase shift δ_l is

$$k^{2l+1} \cot \delta_l = \sum_m \gamma_m \left(\frac{E_p}{10} \right)^m, \quad (1)$$

where l is the orbital angular momentum, k is the nonrelativistic c.m. momentum in F^{-1} , E_p is the proton laboratory kinetic energy in MeV, and γ_m are the coefficients to be varied to fit the data.

At energies where both differential cross sections and polarization are available, we did "single-energy" analyses with the following energy parametrization:

$$\delta(E_p) = \delta(E'_p) + \Delta(E_p - E'_p),$$

where $\delta(E'_p)$ is the value of the phase shift at E_p

$= E'_p$. The slope Δ was kept constant while $\delta(E'_p)$ was varied.

Equations relating the phase shifts to the observables and the electromagnetic corrections are given in Ref. 2. The least-squares search procedure is given in detail in Ref. 3 and is summarized here:

The function to be minimized in the analysis is χ^2 , given by

$$\chi^2 = \sum_n \left[\sum_i \frac{[x_n \theta_i(p) - \theta_i^{\text{exp}}]^2}{(\Delta \theta_i)^2} + \left(\frac{x_n - 1}{\Delta x_n} \right)^2 \right],$$

where

$\theta_i(p)$ = observable (cross section or polarization) as calculated from the variable parameters (p),

θ_i^{exp} = experimental observable,

$\Delta \theta_i$ = experimental error,

x_n = normalization constant for the n th experiment,

and

Δx_n = normalization error for the n th experiment.

The summation on n is over experiments, while the summation on i is over measurements within the n th experiment. The parameters (p) are either the phase shifts, in the case of a single-energy analysis, or the parameters from which the partial-wave amplitudes are derived, in the case of an energy-dependent analysis.

Both the parameters (p) and the normalization factors (x_n) are varied in the analysis to minimize

TABLE I. Energy-dependent parameters for fits to single-energy phase shifts.

l_{2J}	m	Solution A γ_m	Solution B γ_m	Solution	No. of data	No. of parameters	χ^2_{expected}	χ^2
S_1	0	-0.6957	-0.7283	A	24	3	21	70.4
	1	0.6511	0.4911	B	14	3	11	71.1
	2	-0.1527	-0.071 03					
P_1	0	0.1238	0.1333	A	25	4	21	55.8
	1	-0.088 89	-0.1102	B	20	4	16	26.1
	2	0.073 26	-0.008 046					
	3	0.011 01	0.060 67					
P_3	0	0.060 14	0.052 79	A	21	4	17	41.3
	1	-0.2757	-0.2136	B	20	4	16	74.0
	2	0.2403	0.096 53					
	3	-0.060 39	-0.005 06					
D_3	0	-1.000	2.922	A	14	1	13	43.3
				B	15	1	14	44.5
D_5	0	-1.644	2.283	A	13	1	12	2.2
				B	16	1	15	64.8

χ^2 . The algorithm for minimization is successive linearization of the expression for $\theta_i(p)$; that is, assume that $\theta_i(p)$ can be expanded to first order in the parameter increments (Δp):

$$\theta_i(p + \Delta p) = \theta_i(p) + \sum_j \frac{\partial \theta_i}{\partial p_j} \Delta p_j;$$

when this approximation is used in the expression for χ^2 the value of Δp which minimizes χ^2 can be found through a suitable matrix inversion, and the procedure is then repeated until minimization is complete. The normalization parameters are

handled essentially in the same way as are the variable parameters (p), although advantage is taken of the fact that $\partial^2 \chi^2 / \partial x_n \partial x_m$ is a diagonal matrix, thereby allowing us to work in a space whose dimensionality is that of the parameter vector (p). The details of this procedure are given in Ref. 3.

INPUT PARAMETERS

The p - α phase shifts available at the beginning of this investigation essentially were two different solutions, which we call solutions A and B. We

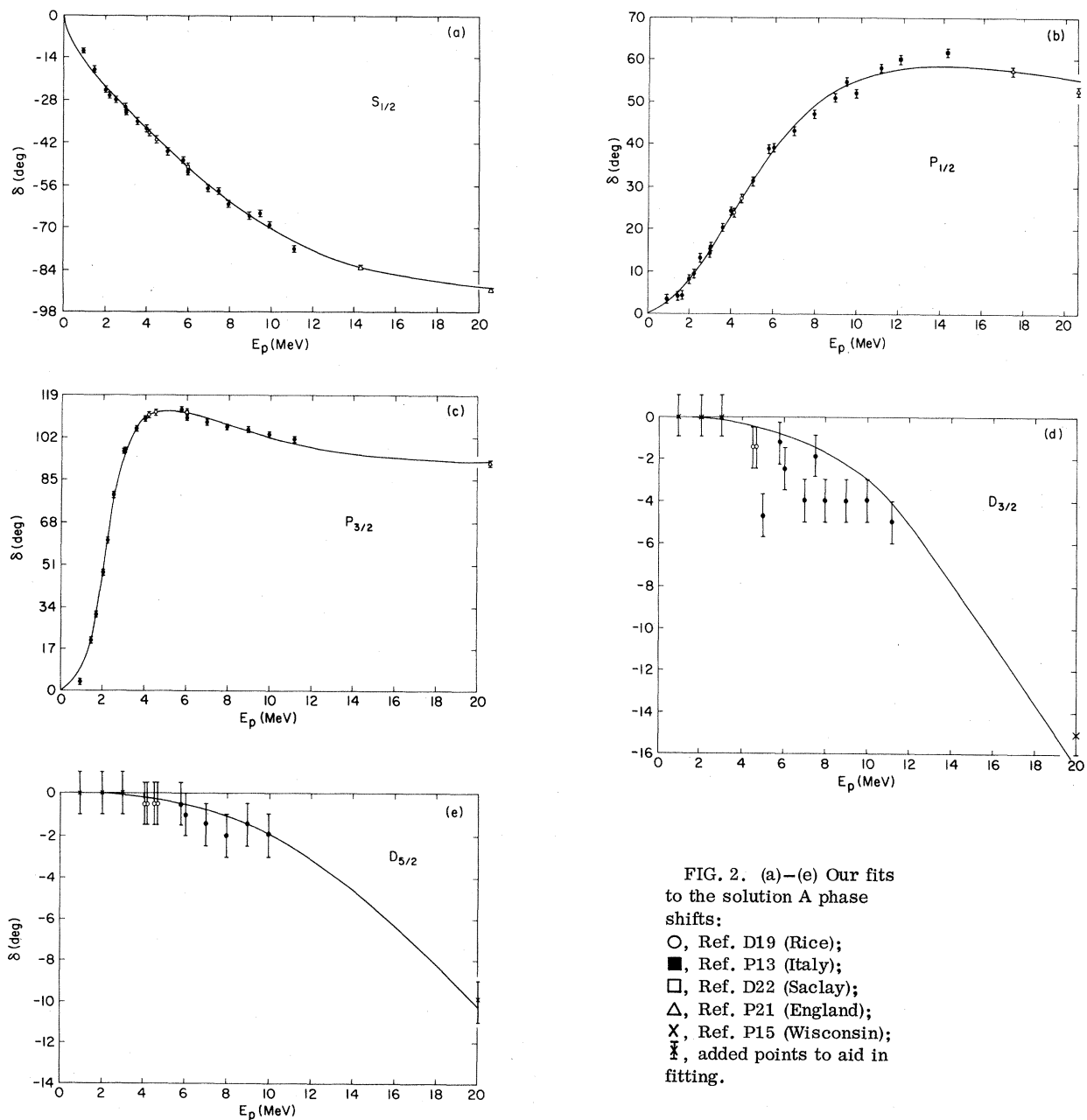


FIG. 2. (a)–(e) Our fits to the solution A phase shifts:
 O, Ref. D19 (Rice);
 ■, Ref. P13 (Italy);
 □, Ref. D22 (Saclay);
 △, Ref. P21 (England);
 X, Ref. P15 (Wisconsin);
 ⌘, added points to aid in fitting.

fit our energy-dependent form to the available phase shifts and thereby obtained the parameters shown in Table I. Our energy-dependent fit is shown along with the input phases for solution A in Fig. 2 and for solution B in Fig. 3. These two solutions' parameters were used as input in fitting all of the elastic scattering data from 0 to 22 MeV.

RESULTS

A. Energy-Dependent Analyses

The results of our energy-dependent analyses are shown in Table II. The first two solutions are

started from our fits to the available single-energy phase shifts. Although neither of these fits is exceptionally good, starting from the solution B phases seemed to achieve better agreement with the entire set of 0–22-MeV experimental data. This was apparently because solution B had positive D waves, whereas solution A had negative D waves. The $P_{1/2}$ phase ended up more like the solution A input phase for both fits. Several experiments were very poorly fitted by both solutions. Also, the solution-B phases changed less upon searching than did the solution-A phases, except for $P_{1/2}$. For example, the solution-A negative

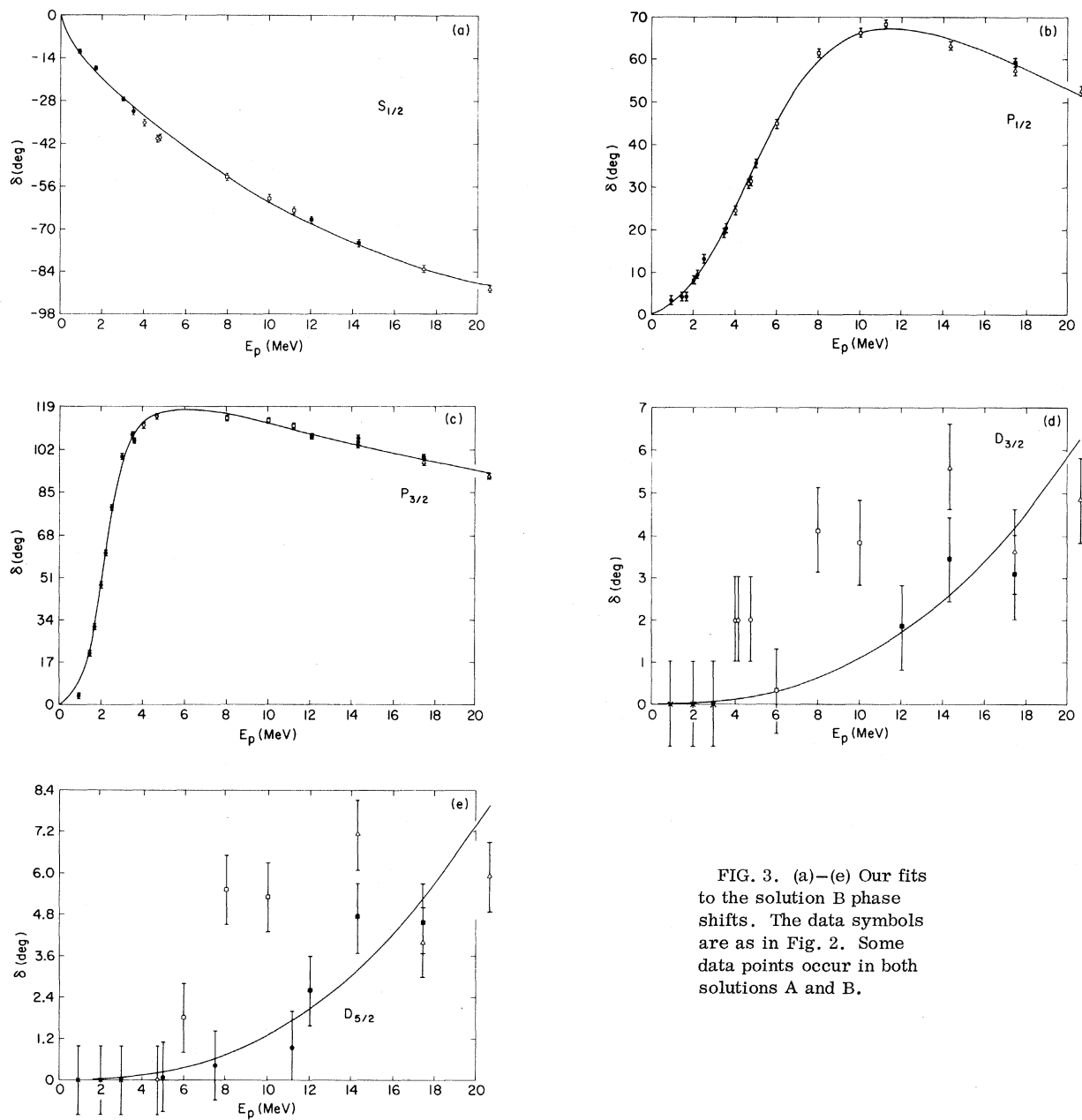


FIG. 3. (a)–(e) Our fits to the solution B phase shifts. The data symbols are as in Fig. 2. Some data points occur in both solutions A and B.

TABLE II. Energy-dependent analyses.

Solution no.	No. of data	Input solution	Phases searched	No. of parameters	Expected χ^2	χ^2	$\chi^2/\chi^2_{\text{expected}}$	Special features of result
0-22 MeV								
1	1327	A	<i>SPD</i>	13	1314	3345	2.55	Negative <i>D</i> waves become small; $D_{3/2} < D_{5/2}$
2	1327	B	<i>SPD</i>	13	1314	3104	2.37	$0 < D_{3/2} < D_{5/2}$
3	1327	Single energy	<i>SPD</i>	14	1313	3006	2.29	$0 < D_{3/2} < D_{5/2}$
4	1327	3	<i>SPDF</i>	16	1311	2927	2.24	$F_{5/7} < F_{7/2} \approx 3^\circ$ at 22 MeV
5	1327	3	<i>SPDF</i>	17	1310	2930	2.24	Extra $D_{3/2}$ parameter did not change solution 3
6	1327	4	<i>SPDF</i>	17	1311	2927	2.24	Extra $D_{3/2}$ parameter did not change solution 4
7	1327	3	<i>SPDF</i>	17	1310	2923	2.23	Extra $D_{3/2}$ did not change solution 3
8	1327	3	<i>SPDF</i>	18	1309	2860	2.18	2 parameters in both <i>D</i> waves $D_{3/2} \approx 10, D_{5/2} \approx 13$ at 22 MeV
9	1327	8	<i>SPD</i>	16	1311	2950	2.25	<i>D</i> waves lowered about 2°
10	1201	8	<i>SPDF</i>	18	1183	1816	1.51	Essentially same as solution 8
0-22.94 MeV								
11	1313	8	<i>SPDF</i>	18	1295	2101	1.62	See Fig. 4
12	1313	Single energy	<i>SPDF</i>	21	1292	2096	1.62	Essentially same as solution 11
13	1343	11	<i>SPDF</i>	14	1329	1952	1.47	Correct low-energy parametrization

TABLE III. Single-energy analyses result at energies where both differential-cross-section and polarization data are available. Details of the fits are available in a report VPISA-1(70) from the authors.

Energy (MeV)	$s_{1/2}$	$P_{1/2}$	$P_{3/2}$	$D_{3/2}$	$D_{5/2}$	$F_{5/2}$	$F_{7/2}$	No. of data	χ^2
0.94	-10.5 ± 0.39	0.508 ± 0.36	5.02 ± 0.32	22	10.9
1.49	-18.3 ± 0.60	4.31 ± 0.65	20.05 ± 0.45	23	22.0
1.70	-22.6 ± 0.85	7.56 ± 0.68	28.15 ± 0.72	23	31.6
1.97	-22.9 ± 0.77	7.17 ± 0.36	47.46 ± 0.57	49	72.9
2.18	-26.02 ± 1.48	9.217 ± 0.42	57.87 ± 1.50	24	8.98
2.53	-28.33 ± 1.40	12.32 ± 0.66	78.06 ± 1.55	18	8.52
3.006	-30.41 ± 0.40	15.01 ± 0.30	96.71 ± 0.518	39	77.0
3.47	-33.14 ± 1.76	22.29 ± 2.34	106.7 ± 2.12	16	3.56
4.006	-38.06 ± 0.38	24.57 ± 0.41	108.7 ± 0.49	44	89.1
4.5	-40.14 ± 1.39	29.91 ± 0.66	113.2 ± 1.43	33	10.5
6.02	-47.47 ± 0.32	42.94 ± 0.27	114.2 ± 0.37	47	73.1
7.967	-55.57 ± 0.30	52.56 ± 0.35	111.92 ± 0.40	42	66.7
8.5	-57.67 ± 0.57	54.61 ± 0.88	111.06 ± 0.98	38	79.5
9.89	-64.37 ± 0.75	54.41 ± 0.74	106.44 ± 0.75	53	53.1
9.89	-62.89 ± 0.33	56.14 ± 0.38	107.91 ± 0.44	46	61.2
10.00	-62.57 ± 0.78	56.85 ± 1.2	108.43 ± 1.3	33	57.2
11.16	-74.55 ± 1.6	53.50 ± 1.3	97.48 ± 1.72	-0.41 ± 0.77	2.17 ± 0.4	27	134.0
12.04	-71.42 ± 0.2	53.35 ± 0.71	101.39 ± 0.47	-0.90 ± 0.26	-0.90 ± 0.35	82	91.0
14.23	-77.97 ± 0.51	53.54 ± 1.2	97.32 ± 0.96	-0.34 ± 0.58	0.11 ± 0.73	50	37.4
17.45	-80.00 ± 1.00	60.20 ± 1.22	99.81 ± 1.1	3.29 ± 0.53	5.05 ± 0.64	0.88 ± 0.23	1.20 ± 0.28	80	165.4
22.15	-87.56 ± 3.64	53.60 ± 3.27	91.73 ± 3.32	7.96 ± 1.28	7.78 ± 1.54	1.97 ± 0.67	2.41 ± 0.81	24	11.9
22.41	-89.55 ± 3.33	50.58 ± 2.99	86.78 ± 3.11	6.96 ± 1.10	6.13 ± 1.38	1.43 ± 0.60	2.27 ± 0.74	24	28.6
22.7	-94.03 ± 3.52	48.84 ± 3.16	86.23 ± 3.56	8.76 ± 1.12	6.63 ± 1.36	1.76 ± 0.59	2.20 ± 0.73	24	7.31
22.93	-94.00 ± 2.22	51.63 ± 2.33	92.38 ± 2.72	13.42 ± 1.13	9.37 ± 1.13	1.33 ± 0.54	2.54 ± 0.61	24	52.9
23.06	-93.09 ± 3.37	51.77 ± 2.79	89.60 ± 2.34	15.12 ± 1.41	8.54 ± 1.27	0.68 ± 0.85	1.24 ± 0.78	24	11.0

D waves converged to almost zero.

We used solution 2 of Table II as input in single-energy analyses at energies where both differential cross sections and polarization data were available. The results are given in Table III.

In an attempt to find a better energy-dependent solution without culling more data, we converted the single-energy S - and P -wave results to $k^{2l+1}\cot\delta_l$ and fit to our parametrization, Eq. (1). These parameters were then used as input to obtain solution 3 of Table II. In solutions 4 through 8, F waves were added. Only one parameter was used in them. The D waves in solution 4 had only one parameter; in solution 5 through 7 the $D_{3/2}$ phase had two parameters; in solution 8 both D waves had two parameters. The D waves increased considerably (solution 8) when the number of D -wave parameters for both was increased to two. In solution 9 we tried to see if the F waves were necessary to achieve a good fit. Comparison with solution 8 shows that they significantly improve the fit. We discarded all experiments that gave an average χ^2 per datum of 4 or greater⁴ and obtained solution 10, which is essentially the same as solution 8.

Near threshold for the inelastic reaction $p + \alpha \rightarrow d + \text{He}^3$ ($E_{\text{th}} = 23.02$ MeV) we expect that the $D_{3/2}$ phase may vary rapidly because of the Li^5 resonance just above threshold. After obtaining the 0–22-MeV solutions we extended our analysis to 22.94 MeV by starting from the last 0–22-MeV solution (solution 10). We thereby obtain solution 11 of Table II. We, also, did single-energy analyses at energies where both differential cross sections and polarization data are available, the re-

sults are shown in Table III. Then we fit our parametrization to the single-energy results and redid the energy-dependent analysis, which is solution 12 of Table II. Solutions 11 and 12 are essentially the same. They represent the best 0–23-MeV solution we achieved with the parametrization given by Eq. (1).

We then introduced a new parametrization in an effort to improve the fit. This more complicated form is discussed by Preston.⁵ It adds a correction for Coulomb-barrier penetration. The corrected equation is

$$C_l^2(\eta)k^{2l+1} \left[\cot\delta_l + \frac{2\eta h(\eta)}{C_0^2(\eta)} \right] = \sum_m \gamma_m \left(\frac{E_p}{10} \right)^m, \quad (2)$$

where

$$\eta = 2 \frac{M_p M_\alpha}{M_p + M_\alpha} \frac{e^2}{\hbar^2 k},$$

$$C_0^2(\eta) = 2\pi\eta / (e^{2\pi\eta} - 1),$$

$$C_l^2(\eta) = C_{l-1}^2(\eta)(1 + \eta^2/l^2),$$

$$h(\eta) = \eta^2 \sum_{s=1}^{\infty} \frac{1}{S(S^2 + \eta^2)} - \ln\eta - \gamma,$$

and

$$\gamma = 0.577216 \text{ (Euler's const.)}.$$

As k increases $C_l(\eta) \rightarrow 1$ and $h(\eta) \rightarrow 0$, so Eq. (2) approaches the original parametrization [Eq. (1)]. Using this form we analyzed the original data set, discarding only the redundant and inconsistent data listed in the section "Data." We did the analyses in three steps, 0–10, 0–17.45, and 0–22.94 MeV. Again we discarded all experiments⁶ giving average χ^2 per datum greater than 4. We thereby obtained solution 13 of Table II. In Fig. 4 we plot solutions 11 and 13 of Table II. We consider solution 13 as our best solution to all of the 0–23-MeV p - α data. In Table IV we give the parameters for solution 13 of Table II, and in Table V we list selected values of the solution 13 phase shifts.

B. Single-Energy Analyses

Our main purpose in this work is to obtain energy-dependent solutions for the p - α phase shifts. However, for the following three reasons we did single-energy analyses starting from the best energy-dependent solution (solution 2 of Table II) obtained after initially searching from solutions A and B: (1) To indicate the erratic behavior with energy of single-energy analyses; (2) to indicate the uncertainty in our energy-dependent results; but yet, (3) to indicate how an energy-dependent solution is some sort of average of the erratic single-energy results. The results are given in Table III and are plotted in Fig. 4.

TABLE IV. Fit parameters for solution 13 of Table II.

l_{2j}	m	γ_m	$\Delta\gamma_m^a$
S_1	0	-0.2117	0.0019
	1	0.2093	0.0021
P_1	0	0.069 43	0.000 78
	1	-0.035 27	0.0020
	2	0.109 1	0.0013
P_3	0	0.022 46	0.000 11
	1	-0.057 31	0.000 62
	2	0.056 57	0.000 59
D_3	0	24.64	0.70
	1	-9.867	0.31
D_5	0	7.510	0.23
	1	-2.157	0.13
F_5	0	9.154	0.95
F_7	0	6.596	0.57

^a $\Delta\gamma_m$ is the change in γ_m that changes χ^2 by 1 when all other parameters are searched.

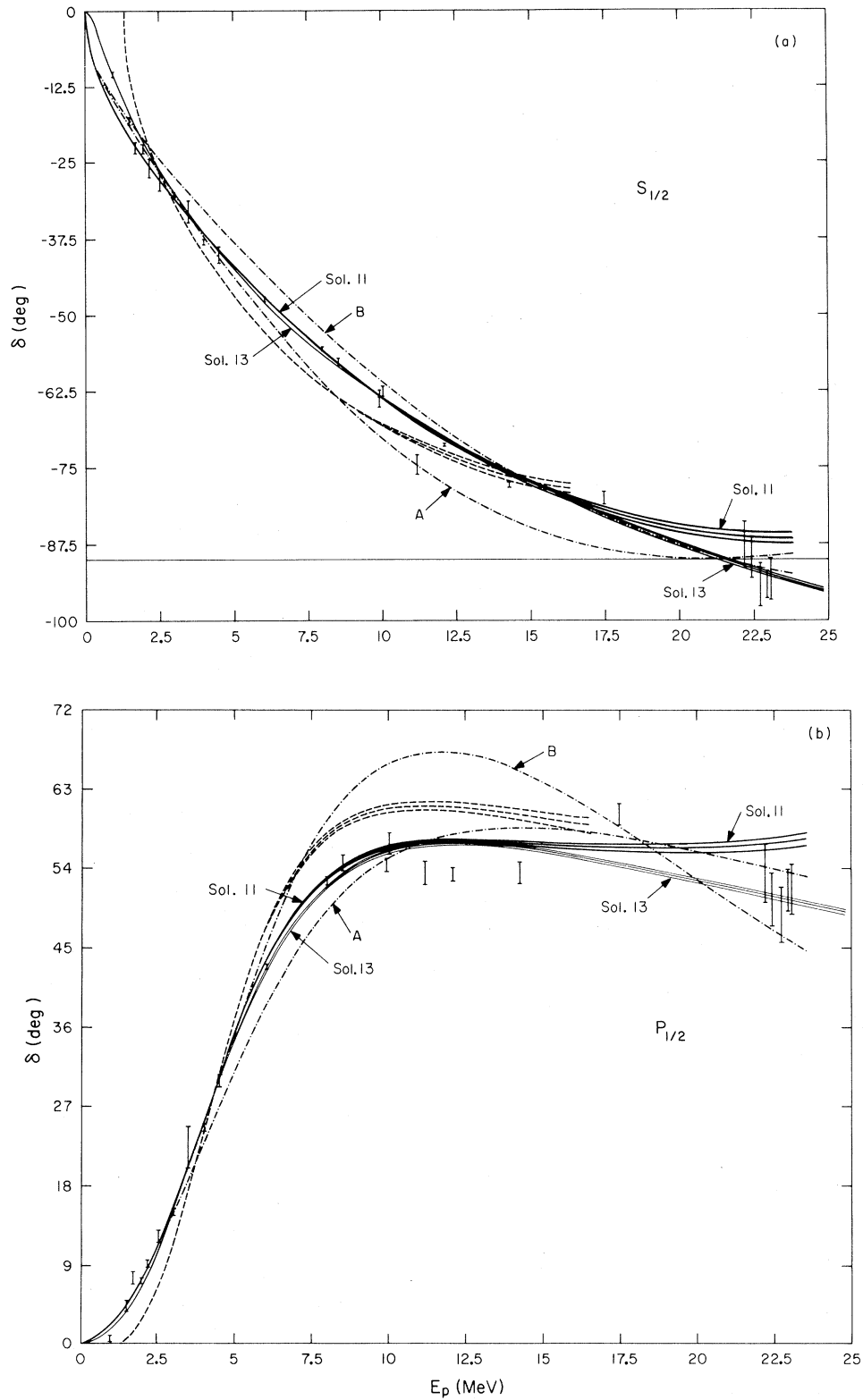


FIG. 4. (a), (b) Solutions 11 and 13 of Table II. The data points are the single-energy values of Table III. The input solutions (A and B) are indicated by dot-dash lines. Our previous $n-\alpha$ solution (Ref. 1) appropriately shifted up to 1.29 MeV is indicated by dashed lines. [Figure 4 contains seven parts. Parts (c), (d), (e), and (f) of Fig. 4 are shown on following pages.]

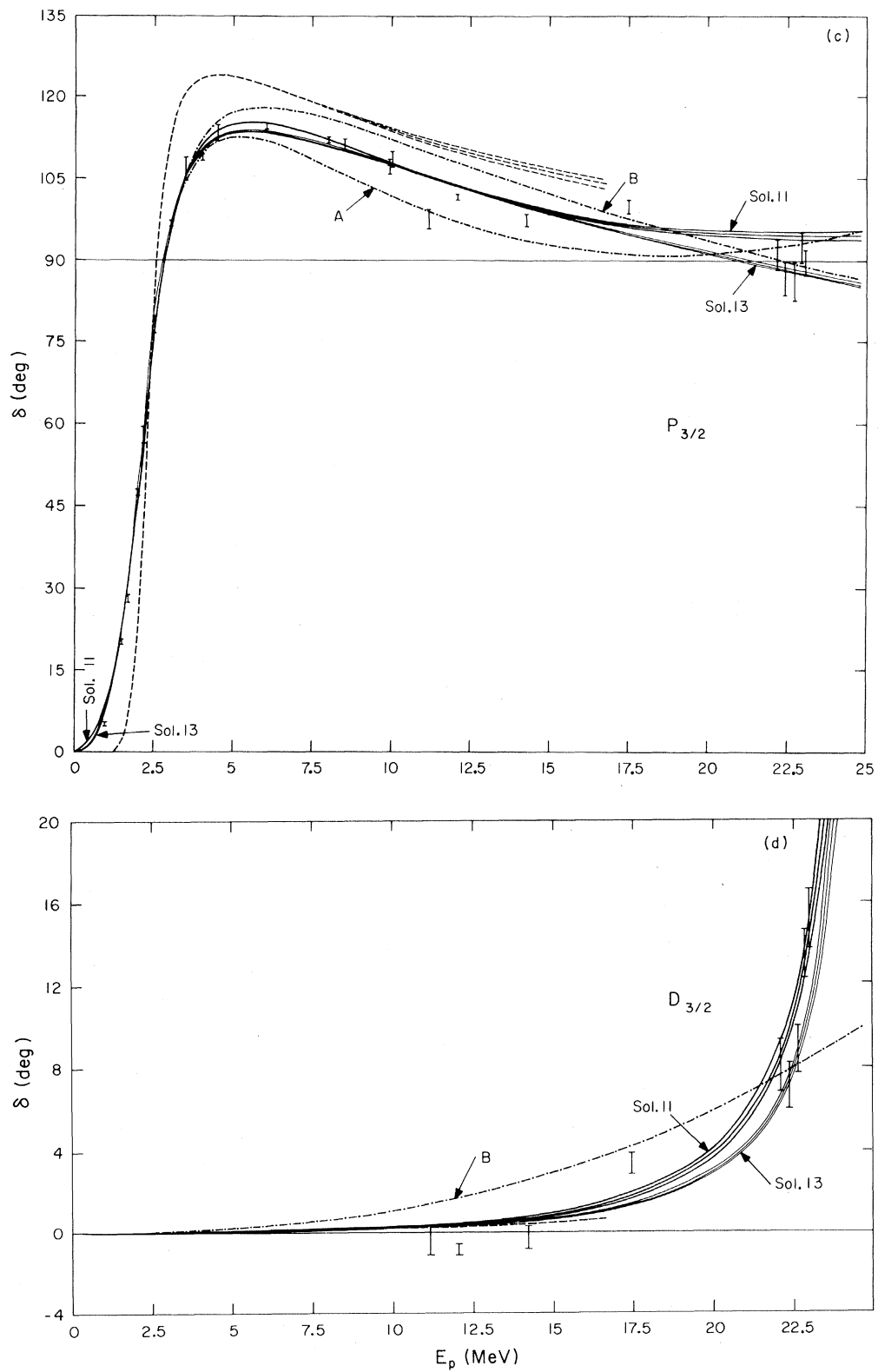


FIG. 4. (c), (d) Solutions 11 and 13 of Table II. The data points are the single-energy values of Table III. The input solutions (A and B) are indicated by dot-dash lines. Our previous $n-\alpha$ solution (Ref. 1) appropriately shifted up to 1.29 MeV is indicated by dashed lines.

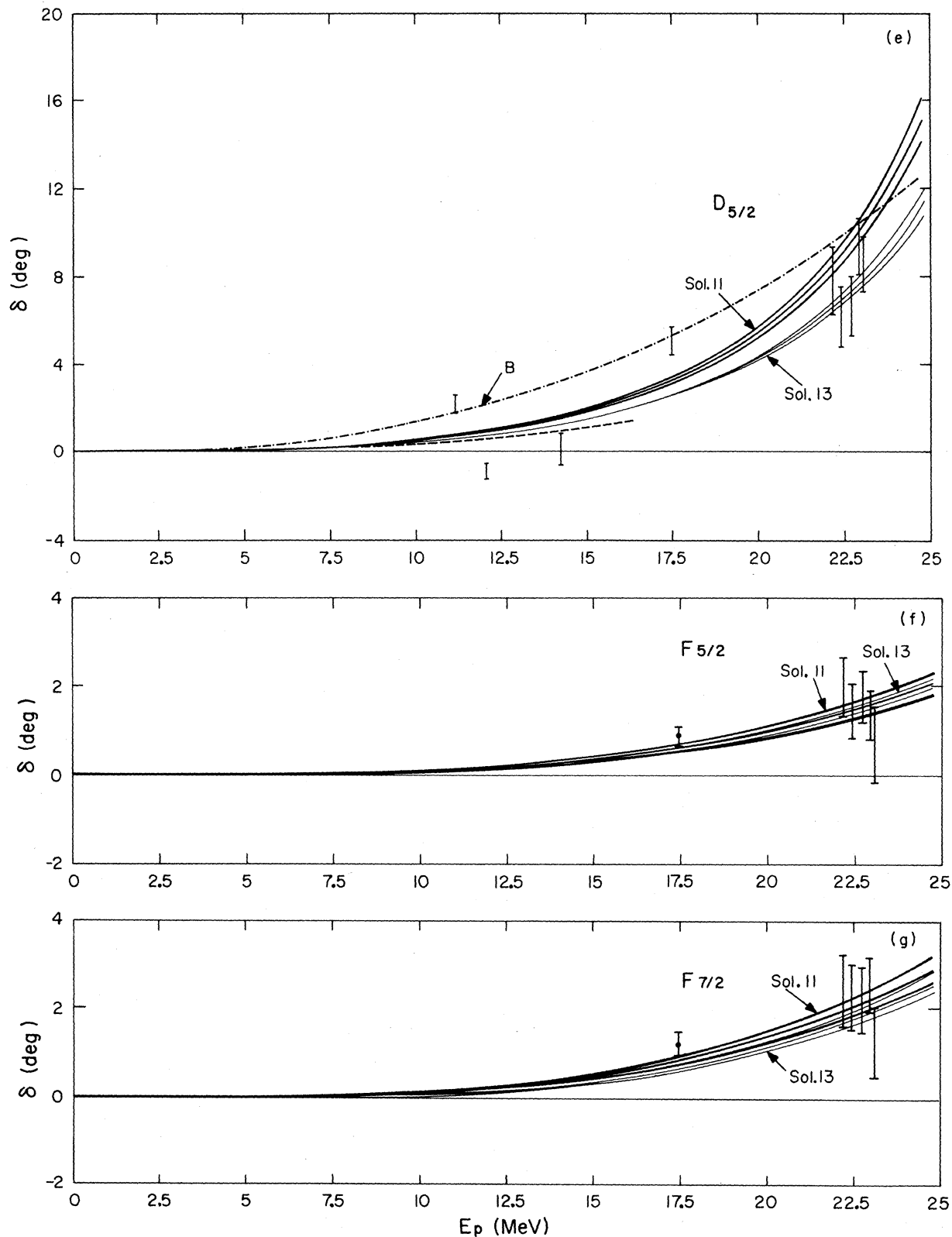


FIG. 4. (e)-(g) Solutions 11 and 13 of Table II. The data points are the single-energy values of Table III. The input solutions (A and B) are indicated by dot-dash lines. Our previous n - α solution (Ref. 1) appropriately shifted up to 1.29 MeV is indicated by dashed lines.

We have made no attempt to find unique single-energy solutions by starting from random inputs.

CONCLUSION

The many inconsistencies in the data make it impossible to obtain low values of χ^2 in the energy-dependent analysis (see Table II).

In Fig. 4 we show our previous $n-\alpha$ solution¹ along with our $p-\alpha$ solutions 11 and 13 of Table II.

The effect of the Coulomb-barrier-penetration correction can be seen by comparing the low-energy behavior of solutions 11 and 13. It appears that using the correct low-energy structure in solution 13 allowed the high-energy phases to search to values closer to our single-energy results. The $n-\alpha$ solution has been shifted up 1.29 MeV in order that the c.m. energy is the same in both $n-\alpha$ and $p-\alpha$ systems. From this comparison we must conclude that although the gross features are the

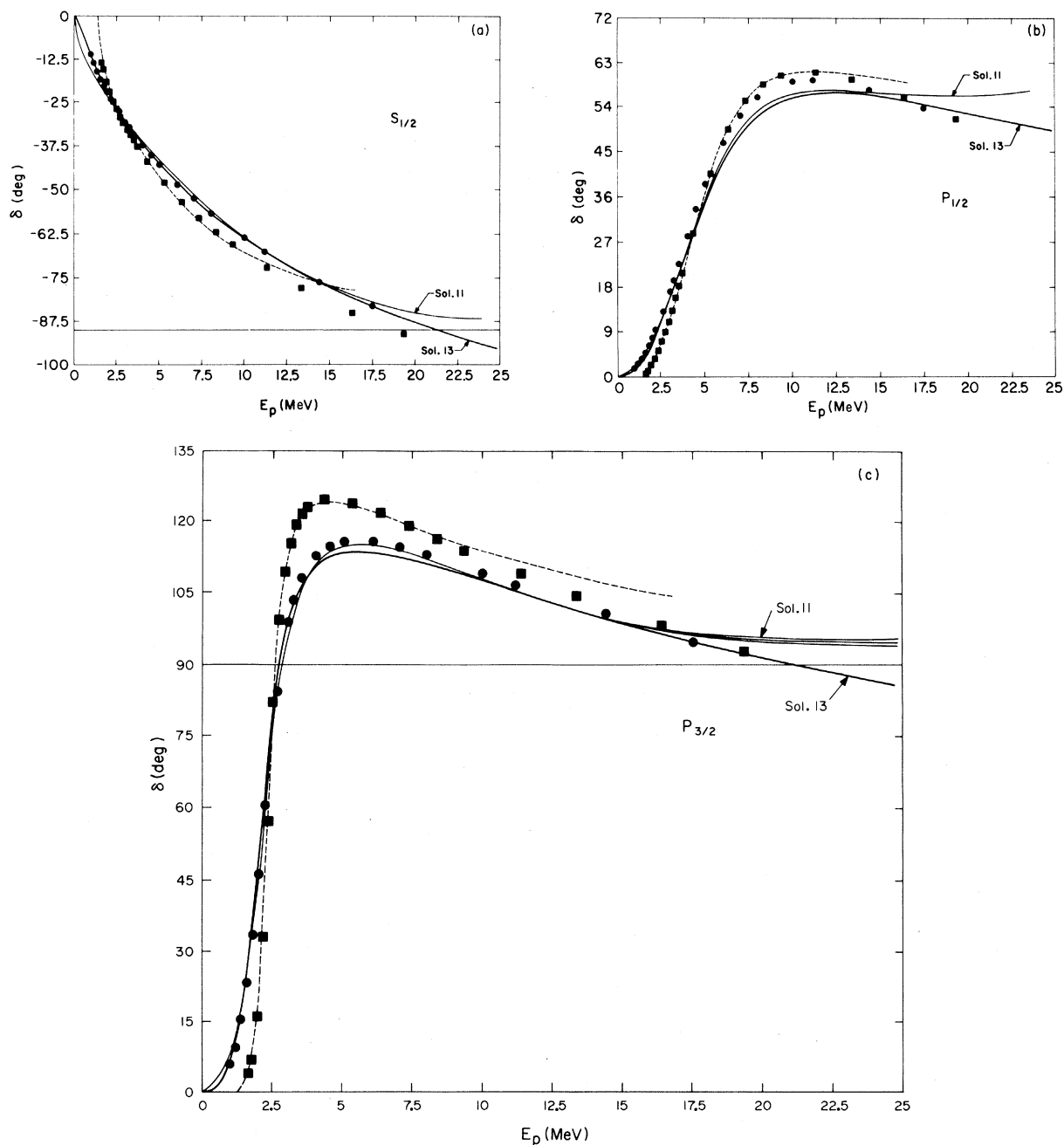


FIG. 5. (a)–(c) Solution 13 of Table II. Our previous $n-\alpha$ solution (Ref. 1) appropriately shifted up to 1.29 MeV is indicated by a dashed line. ●, Satchler's $p-\alpha$ phases (Ref. 4); ■, Satchler's $n-\alpha$ phases (Ref. 4).

TABLE V. Values of phase shifts at selected energies for solution 13 of Table III.

Energy (MeV)	Phase (deg)						
	$S_{1/2}$	$P_{1/2}$	$P_{3/2}$	$D_{3/2}$	$D_{5/2}$	$F_{5/2}$	$F_{7/2}$
0.940	-10.988	1.458	6.175	0	0	0	0
2.020	-22.308	7.120	50.774	0.001	0.004	0	0
2.510	-26.470	10.921	79.767	0.002	0.007	0	0.001
3.006	-30.270	15.378	97.313	0.004	0.012	0.001	0.001
4.006	-36.993	25.349	110.376	0.009	0.028	0.002	0.003
5.011	-42.812	35.005	113.398	0.017	0.053	0.006	0.008
6.016	-47.937	42.849	113.418	0.030	0.090	0.011	0.016
7.500	-54.544	50.530	111.611	0.059	0.172	0.026	0.035
8.500	-58.484	53.583	109.944	0.087	0.250	0.040	0.056
10.000	-63.780	56.049	107.251	0.148	0.409	0.073	0.102
12.040	-70.032	57.008	103.588	0.280	0.731	0.145	0.201
13.650	-74.348	56.731	100.828	0.447	1.098	0.229	0.318
15.050	-77.739	56.102	98.551	0.660	1.525	0.326	0.453
17.840	-83.673	54.335	94.364	1.442	2.794	0.605	0.841
19.960	-87.584	52.817	91.476	2.773	4.317	0.910	1.265
20.870	-89.130	52.156	90.308	3.828	5.188	1.069	1.488
22.000	-90.983	51.339	88.914	6.132	6.516	1.295	1.803
22.600	-91.877	50.910	88.150	8.322	7.358	1.428	1.988
22.940	-92.390	50.668	87.799	10.175	7.886	1.508	2.099

same in the n - α and p - α systems, the details are quite different over most of the elastic energy range.

We have compared our p - α solutions 11 and 13 and our previous n - α solution with the p - α and n - α phases obtained from the optical model by Satchler *et al.*⁷ Figure 5 shows the Satchler S - and P -wave phases plotted with our solutions. The D -wave optical-model phases (not shown) are in better (but not good) agreement with input solution B than with either solution 13 or our n - α solution.

It is interesting to note that around 10 to 12 MeV our single-energy $P_{1/2}$ phase is lower than our en-

ergy-dependent value, whereas, the Satchler $P_{1/2}$ phase is higher than our energy-dependent value.

We present solution 13 of Table II as our best fit to p - α scattering data from 0 to 23 MeV. We have facilities to plot observables at any energy and angle with errors as predicted by our solution, and would be glad to do so upon request. Also, the listing of the complete data set and the data selection used in our analyses is available.

ACKNOWLEDGMENTS

Dr. Brian DeFacio contributed to the early phases of this work. Several experimentalists have kindly answered questions about their data.

APPENDIX. DATA REFERENCES (0–30 MeV)

Differential Cross Sections

- | | |
|---|---|
| D1. J. Chadwick and E. S. Bieler, <i>Phil. Mag.</i> 42 , 923 (1921) (data not in a useable form). | D7. B. Cork and W. Hartsough, <i>Phys. Rev.</i> 96 , 1267 (1954): 9.73 MeV (17.2–154.3° c.m.). |
| D2. G. Freier, E. Lampi, W. Sleator, and J. H. Williams, <i>Phys. Rev.</i> 75 , 1345 (1949): 0.95, 1.49, 1.70, 2.02, 2.22, 2.53, 3.04, and 3.58 MeV (12.6–168.03° c.m., not full angle range at all energies). | D8. R. G. Freemantle, T. Grottdal, W. M. Gibson, R. McKeague, D. J. Prowse, and J. Rotblat, <i>Phil. Mag.</i> 45 , 1090 (1954): 9.55 MeV (22–167° c.m., data in graph form). |
| D3. C. H. Braden, <i>Phys. Rev.</i> 84 , 762 (1951): 4.8 MeV (30° lab), and 5.1 MeV (30–150° lab). | D9. J. H. Williams and S. W. Rasmussen, <i>Phys. Rev.</i> 98 , 56 (1955): 9.76 MeV (43.3–174.4° c.m.) (apparently Table I incorrectly lists the energy as 9.74 MeV). |
| D4. T. M. Putman, <i>Phys. Rev.</i> 87 , 932 (1952): 9.48 MeV (12.3–174.2° c.m.) (superceded by Ref. D12). | D10. K. W. Brockman, <i>Phys. Rev.</i> 102 , 391 (1956): 17.45 MeV (6.4–168° c.m.). |
| D5. B. Cork, <i>Phys. Rev.</i> 89 , 78 (1952): 19.5 MeV (55° c.m.), and 31.6 MeV (17.1–62.5° c.m.). | D11. R. A. Vanetsian and E. D. Fedchenko, <i>Zh. Eksperim. i Teor. Fiz.</i> 30 , 577 (1956) [transl.: <i>Soviet Phys. - JETP</i> 3 , 624 (1956)]: 18.7 MeV (data not |
| D6. W. E. Kreger, W. Jentschke, and P. G. Kruger, <i>Phys. Rev.</i> 93 , 837 (1953): 5.78 MeV (16.1–154.1° c.m.). | |

- in a useable form).
- D12. T. M. Putman, J. E. Brolley, Jr., and L. Rosen, Phys. Rev. 104, 1303 (1956): 7.5 and 9.48 MeV recalculation of data in Ref. D4 (12.5–174.4° c.m.).
- D13. A. F. Wickersham, Jr., Phys. Rev. 107, 1050 (1957): 28.0 MeV (data not in usable form).
- D14. W. M. Gibson, D. J. Prowse, and J. Rotblat, Proc. Phys. Soc. 243, 237 (1957): 9.55 MeV (actual data given in Ref. D8).
- D15. K. W. Brockman, Jr., Phys. Rev. 108, 1000 (1957): 11.42, 11.65, 12.49, 12.58, 13.3, 13.65, 14.38, 14.49, 15.05, 16.24, 16.76, and 17.84 MeV (36.7–169° c.m.), not full angle range at all energies).
- D16. P. D. Miller and G. C. Phillips, Phys. Rev. 112, 2043 (1958): 3.03, 3.51, 4.02, 4.5, and 5.0 MeV (30–168° c.m.).
- D17. J. W. Burkig, Phys. Rev. 116, 674 (1959): 20.1 MeV (8.7–87.1° c.m.).
- D18. J. Sanada, J. Phys. Soc. Japan 14, 1463 (1959): 12.04 and 14.32 MeV (9.8–153.4° c.m.).
- D19. A. C. L. Barnard, C. M. Jones, and J. L. Weil, Nucl. Phys. 50, 604 (1964): 1.997, 3.006, 4.006, 5.011, 6.016, 6.977, 7.967, 8.96, 9.954, and 11.157 MeV (25.1–164.4° c.m., errors not listed, 1% errors assumed).
- D20. P. Darriulat, D. Garreta, A. Jarrats, and J. Testoni, Nucl. Phys. A108, 316 (1968): 22.15, 22.41, 22.74, 22.93, 23.06, 23.15, 23.25, 23.38, 23.59, 23.85, 24.04, 24.25, and 24.78 MeV (25–161.2° c.m.).
- D21. P. W. Allison and R. Smythe, Nucl. Phys. A121, 97 (1968): 20.03 to 27.68 MeV (7.5–174.03° c.m., not full angle range at all energies).
- D22. D. Garreta, J. Sura, and A. Jarrats, Nucl. Phys. A132, 204 (1969): 12.04, 14.23, and 17.45 MeV (25.0–161.2° c.m.).
- Polarization**
- P1. N. P. Heydenburg and R. B. Roberts, Phys. Rev. 56, 1092 (1939): 0.994 MeV (data not in usable form).
- P2. N. P. Heydenburg and N. F. Ramsey, Phys. Rev. 60, 42 (1941): 1 to 3 MeV (data not in useable form).
- P3. M. Heusinkveld and G. Freier, Phys. Rev. 85, 80 (1952): 3.25 and 3.5 MeV (data not in useable form).
- P4. A. C. Juveland and W. Jentschke, Z. Physik 144, 521 (1956): 5.32 MeV (55° c.m.).
- P5. M. J. Scott, Phys. Rev. 110, 1398 (1958): 1.375 MeV, 73.6° c.m.; 2.02 MeV (73.6° c.m.), and 3.58 MeV, 104.5° c.m.
- P6. J. Sanada, K. Nisimura, S. Suwa, I. Hayashi, K. Fukunga, N. Ryu, and M. Seki, J. Phys. Soc. Japan 15, 754 (1960): 6.2 MeV c.m. (130° c.m.), 9.1 MeV c.m. (61.1° c.m.), and 11.5 MeV c.m. (61.1° c.m.).
- P7. L. Rosen, J. E. Brolley, Jr., and L. Stewart, Phys. Rev. 121, 1423 (1961): 10 MeV (33–151.5° c.m.).
- P8. L. Rosen, J. R. Brolley, Jr., M. C. Gursky, and L. Stewart, Phys. Rev. 124, 199 (1961): 8.5 MeV (40–150.5° c.m.).
- P9. L. Rosen and W. T. Leland, Phys. Rev. Letters 8, 379 (1962): 14.5 MeV (37–165° c.m.).
- P10. R. J. Brown, W. Haeberli, and J. X. Saladin, Nucl. Phys. 47, 212 (1963): 3.65, 4.22, 4.56, 4.77, 4.78, 5.43, 5.93, 7.87, 7.89, 9.82, 9.84, 9.89, and 11.90 MeV (45.8–115.1° lab).
- P11. M. K. Craddock, R. C. Hanna, L. P. Robertson, and B. W. Davies, Phys. Letters 5, 335 (1963): 21.9 MeV (45–82.5° lab), 28.8 MeV (20–157.5° lab), 40.0 MeV (20–157.5° lab), 47.7 MeV (20–157.5° lab).
- P12. C. Manduchi, G. C. Nardelli, M. T. Russo-Manduchi, and G. Zannoni, Nucl. Phys. 53, 605 (1964): 4.5 MeV (superceded by Ref. P13).
- P13. L. Drigo, C. Manduchi, G. C. Nardelli, M. T. Russo-Manduchi, and G. Zannoni, Nucl. Phys. 60, 441 (1964): 4.04, 4.16, 4.5, 4.665, and 4.757 MeV (47.5–132.5° lab).
- P14. R. A. Blue and W. Haeberli, Phys. Rev. 137, B284 (1965): 2.13, 2.32, 2.51, 3.01, 3.47, 3.91, and 4.18 MeV (90.4° lab).
- P15. W. G. Weitkamp and W. Haeberli, Nucl. Phys. 83, 46 (1966): 17.47 to 27.06 MeV (55.4–128.2° c.m.).
- P16. L. Drigo, C. Manduchi, G. C. Nardelli, M. T. Russo-Manduchi, G. Tornielli, and G. Zannoni, Nuovo Cimento 42, 363 (1966): 2.38, 2.61, 2.89, 3.22, 3.54, 3.84, 4.15, and 4.46 MeV (52.5–127.5° lab).
- P17. L. Brown and W. Trackslin, Nucl. Phys. A90, 334 (1967): 0.94 to 3.2 MeV (30–140° lab) (left-right asymmetries).
- P18. M. F. Jahns and E. M. Bernstein, Phys. Rev. 162, 871 (1967): 6, 7.891, 9.89, and 11.156 MeV (46.5–114.3° c.m.).
- P19. B. P. Ad'yasevich, V. G. Antonenko, Yu. P. Polunin, and D. E. Fomenko, Yadern Fiz. 5, 933 (1967) [transl.: Soviet J. Nucl. Phys. 5, 665 (1967)]: 0.222, 0.300, 0.390, 0.500, 0.515 MeV (110° c.m.).
- P20. P. Darriulat, D. Garreta, A. Tarrats, and J. Testoni, Nucl. Phys. A108, 316 (1968): 22.15, 22.41, 22.66, 22.93, 23.06, 23.19, 23.32, 23.46, 23.59, 23.72, 23.85, 23.99, 24.25, and 24.78 MeV (25–161.2° c.m.).
- P21. D. J. Plummer, T. A. Hodges, K. Ramavataram, D. G. Montague, and N. S. Chant, Nucl. Phys. A115, 253 (1968): 10 MeV (109.5–121.0° lab).
- P22. D. Garreta, J. Sura, and A. Tarrats, Nucl. Phys. A132, 204 (1969): 12.04, 14.23, and 17.45 MeV (25–161.2° c.m.).
- P23. P. Schwandt, T. B. Clegg, and W. Haeberli, to be published: 4.58, 5.95, 7.89, 9.89, and 11.94 MeV (31–164.2° c.m.).

*Work supported by a grant from the National Science Foundation.

¹R. A. Arndt and L. D. Roper, Phys. Rev. C 1, 903 (1970).

²L. D. Roper, R. M. Wright, and B. T. Feld, Phys. Rev. 138, B190 (1965); L. D. Roper and R. M. Wright, *ibid.* 138, B921 (1965).

³R. A. Arndt and M. H. MacGregor, Methods Compu-

tational Phys. **6**, 253 (1966).

⁴Data discarded are differential cross sections at 0.95, 1.49, 1.70, 11.157, 18.98, and 19.50 MeV and polarizations at 0.300, 0.390, 0.500, 0.515, 4.04, 4.46, 4.665, 4.757, 4.78, 5.43, and 6.00 MeV.

⁵M. A. Preston, *Physics of the Nucleus* (Addison-Wesley Publishing Company, Inc., Reading, Massachusetts,

1962), Appendix B.

⁶Data discarded are differential cross sections at 11.16, 17.45 (D10) and 19.5 MeV and polarizations at 4.46, 4.665, 5.43, 6.00, and 22.93 MeV.

⁷G. R. Satchler, L. W. Owen, A. J. Elwyn, G. L. Morgan, and R. L. Walter, Nucl. Phys. **A112**, 1 (1968).

PHYSICAL REVIEW C

VOLUME 3, NUMBER 6

JUNE 1971

Discussion of a Particular Form of Cluster Wave Functions

F. C. Chang

Physics Department, St. John's University, Jamaica, New York 11432

(Received 18 August 1970; revised manuscript received 10 February 1971)

The meaning of a particular form of cluster wave functions, which have been used in a previous paper to describe the ground-state rotational band of ²⁰Ne, is discussed.

I. INTRODUCTION

Several forms of cluster wave functions have been proposed.¹ In a recent paper² we proposed a form of cluster wave functions which seems to be particularly suited for the nuclei ¹⁹F and ²⁰Ne. With our cluster wave functions the excitation energies of the ground-state rotational band of ²⁰Ne were calculated, and reasonable agreement with the experimental values was obtained. However, what the wave functions actually represent is not evident. It is the purpose of this paper to discuss the meaning of these wave functions.

II. CLUSTER WAVE FUNCTIONS

For ²⁰Ne, cluster wave functions of the following form were used:

$$\Psi(JM) = Na[\Psi(^{16}\text{O})\Psi_\alpha(JM)] = N'a[\Psi(^{16}\text{O})\Psi'_\alpha(JM)]. \quad (1)$$

Here the function $\Psi_\alpha(JM)$ describes an α cluster with total angular momentum J and Z component M moving in a potential well generated by an inert ¹⁶O core. The function $\Psi'_\alpha(JM)$ is obtained from $\Psi_\alpha(JM)$ by deleting terms containing single-particle states occupied by the core nucleons and normalizing. The function $\Psi(^{16}\text{O})$ describes the inert ¹⁶O core. a is an antisymmetrizer. N and N' are normalization constants. It is well known that continual existence of subunits in a nucleus is not allowed by the Pauli principle. In our model of ²⁰Ne the probability of finding an α cluster (in its internal ground state) outside the inert ¹⁶O core is given by

$$P_\alpha = \left| \int \Psi_\alpha^*(JM)\Psi'_\alpha(JM) \right|^2. \quad (2)$$

Since the space part of Ψ_α is taken to be totally symmetric,² the total wave function Ψ_α is a product of a space function and a spin-isospin function:

$$\Psi_\alpha = \psi_\alpha \chi(S=0, T=0), \quad (3)$$

where ψ_α denotes the space function, and $\chi(S=0, T=0)$ denotes a totally antisymmetric spin-isospin function with spin $S=0$ and isospin $T=0$. ψ_α can be expanded in terms of products of single-particle orbital wave functions:

$$\psi_\alpha = \sum_{i=1}^n C_i \psi_i, \quad (4)$$

where C_i are the expansion coefficients. Suppose all terms in (4) with $i > n'$ contain single-particle orbital states occupied by the core nucleons. Then the space part ψ'_α of Ψ'_α is the sum

$$\psi'_\alpha = B \sum_{i=1}^{n'} C_i \psi_i, \quad (5)$$

where $B = (\sum_{i=1}^{n'} |C_i|^2)^{-1/2}$ is a normalization constant. Note that $\Psi'_\alpha = \psi'_\alpha \chi(S=0, T=0)$. Thus we obtain

$$P_\alpha = \sum_{i=1}^{n'} |C_i|^2. \quad (6)$$

The value of P_α was calculated³ to be 3.8% for all states of the ground-state rotational band of ²⁰Ne.

III. DISCUSSION

The smallness of the value of P_α casts doubt on the usefulness of the cluster wave functions (1). In Appendix A we shall show that, for the low-lying states of ²⁰Ne, the wave functions (1) represent states of two protons and two neutrons in the s - d shell with the largest probability of occurrence of